DOI: 10.1002/ejoc.201101384

Synthesis and Characterization of Adducts Formed in the Reactions of Safrole 2′,3′-Oxide with 2′-Deoxyadenosine, Adenine, and Calf Thymus DNA

Li-Ching Shen,[a] Su-Yin Chiang,[b] I-Ting Ho,[a] Kuen-Yuh Wu,*[c] and Wen-Sheng Chung*[a]

Keywords: DNA adducts / DNA damage / Safrole / Cancer

Safrole (**1**) is a natural product found in herbs and spices. Upon uptake, it can be metabolized to safrole 2′,3′-oxide [(±)-SFO, **2**], which can react with DNA bases to form DNA adducts. The reactions of **2** with 2′-deoxyadenosine (**3**) and adenine (**8**) under physiological conditions (pH 7.4, 37 °C) were carried out to characterize its possible adducts with adenine. Four adducts were isolated by reverse-phase liquid chromatography and their structures were characterized by UV/Vis, ^{1}H and ^{13}C NMR spectroscopy and MS. The reaction of **2** with **3** produced two regioisomers, *N*1γ-SFO-dAdo (**4**) and N^6γ-SFO-dAdo (**5**), in 4.2–4.5 % yield, and the reaction of **2** with **8** generated *N*3γ-SFO-Ade (**9**) and *N*9γ-SFO-Ade (**10**) in 1.0–2.4 % yield. Using HPLC–ESI-MS/MS, we traced the amounts of the four adducts formed when calf thymus DNA (10 mg) was treated with **2** (60 μmol) and the levels of **4**, **5**, and **9** were determined to be 2000, 170, and 660 adducts per 10^6 nucleotides, respectively. Adduct **10** was not detected under these conditions. These results suggested that stable DNA adducts of **2** were formed in vitro, and further studies on the formation of these DNA adducts in vivo may help to elucidate their role in safrole carcinogenicity.

Introduction

Safrole (**1**) is a natural product found in herbs and spices, which include basil, cinnamon, nutmeg, ginger, and black pepper.[1] It causes a significant increase of liver cancer in mice and has been classified as a hepatocarcinogen.[2–4] Safrole can also cause chromosomal aberrations, sister chromatid exchanges, and the formation of DNA adducts in hepatocytes of F344 rats.[2] In Taiwan, piper betle inflorescence, which contains 15 mg/g of safrole, is commonly chewed together with areca quid,[5] and the concentration of safrole in saliva has been reported to be as high as 420 μM.[6] Previous studies have shown that areca quid chewing could be a critical risk factor for oral squamous cell carcinoma, oral submucous fibrosis, and esophageal carcinogenesis.[1,6]

Safrole can be metabolized by cytochrome P450 to 1′-hydroxysafrole and safrole 2′,3′-oxide [(±)-SFO, **2**].[7–9] 1′-Hydroxysafrole is enzymatically metabolized by sulfotransferases to 1′-sulfooxysafrole, which can attack DNA bases to form DNA adducts, such as N^2-(*trans*-isosafrol-3′-yl)-2′-deoxyguanosine and N^2-(safrole-1′-yl)-2′-deoxyguanosine.[10] Both of these adducts have been detected by Liu et al. using the ^{32}P-postlabeling method in oral tissues of an oral cancer patient with a history of chewing betle quid.[6] Compound **2** has been shown to have moderate mutagenicity in *Salmonella typhimurium* TA 1535[11,12] and TA 100.[12] Administration of **2** to female CD-1 mice has led to skin tumors.[13] Moreover, **2** exhibits genotoxicity in HepG2 cells and in mice, with evidence of significant increase in the frequencies of DNA strand breaks and micronucleus formation.[14] However, Guenthner et al. have reported that DNA adducts of **2** can be formed in vitro but were not detectable in vivo.[9,15] The structure of **2** is similar to that of many epoxides whose genotoxicity and potential formation of DNA adducts have been well studied,[16–18] which led to our interest in purifying and characterizing potential DNA adducts of **2** in vitro.

Epoxide metabolites frequently attack DNA bases through S_N2 reactions to form DNA adducts at the N^2 and *N*7 positions of guanine and the *N*1, N^6, and *N*3 positions of adenine.[17–20] For example, allylbenzene 2′,3′-oxide has been shown to react with 2′-deoxyguanosine to form N^2-(2′-hydroxy-3′-phenylpropyl)-2′-deoxyguanosine.[9] In order to gain more insight into the genotoxicity of **2**, we needed to synthesize related DNA adducts as standards. However, there have been no reports on the structural characterization of DNA adducts of **2**, thus, our initial objective was to synthesize, purify, and characterize adducts of **2** with 2′-

[a] Department of Applied Chemistry, National Chiao Tung University,
Hsinchu 30050, Taiwan
Fax: +886-3-572-3764
E-mail: wschung@nctu.edu.tw
[b] School of Chinese Medicine, China Medical University,
Taichung 404, Taiwan
[c] Institute of Occupational Medicine and Industrial Hygiene, National Taiwan University,
Taipei, Taipei 106, Taiwan
Fax: +886-2-3366-8077
E-mail: kuenyuhwu@ntu.edu.tw

Supporting information for this article is available on the WWW under http://dx.doi.org/10.1002/ejoc.201101384.

deoxyadenosine and 2′-deoxyguanosine. Our preliminary results showed that the *N*7-guanine adduct was the major product when **2** was treated with 2′-deoxyguanosine or calf thymus DNA (2700 adducts per 10^6 nucleotides, unpublished data). Furthermore, the *N*7-guanine adduct was easily detected in the urine of mice when it was pretreated with **2**. These consequences imply that the genotoxicity of **2** should be of concern because the formation of DNA adducts is the initial stage of gene mutation. As animal studies will take some time, the study of the reaction of **2** with 2′-deoxyguanosine will be reported separately. Here, we report our work on the reactions of **2** with 2′-deoxyadenosine (**3**) and adenine (**8**), which gave four major adducts: *N*1γ-SFO-dAdo (**4**), N^6γ-SFO-dAdo (**5**), *N*3γ-SFO-Ade (**9**), and *N*9γ-SFO-Ade (**10**). The structures of these adducts were characterized by ^{1}H and ^{13}C NMR, heteronuclear multiple quantum coherence (HMQC), and HMBC spectroscopy and MS. HPLC–ESI-MS/MS was used to analyze the adducts generated from the reaction of **2** with calf thymus DNA.

Results and Discussion

Reaction of 2 with 3

The reaction of **2** with **3** at 37 °C for 3 d yielded **4** and **5** in 4.2 and 4.5% isolated yields, respectively (Scheme 2). This reaction was monitored by HPLC, which showed that **4** and **5** appeared at retention times (t_R) of 18.6 and 23.2 min, respectively (Figure 1, a). Unidentified peaks at t_R = 14.2 and 32.1 min were generated when **2** was incubated in the absence of **3** and **8** under the same conditions.

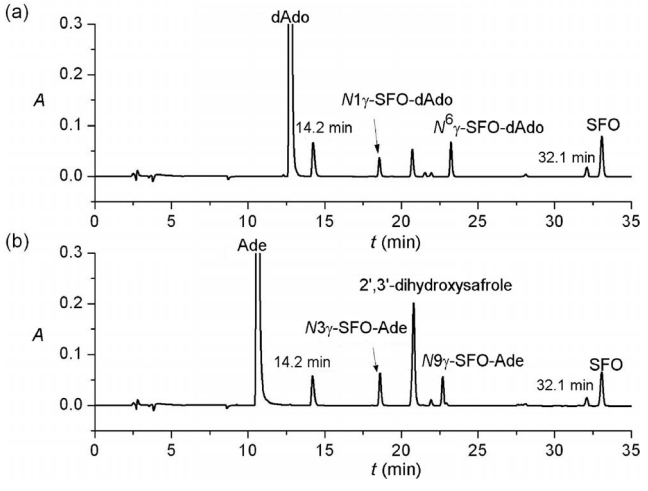

Figure 1. HPLC plots monitored at 260 nm of the reaction mixtures of **2** with (a) **3** and (b) **8** in 0.2 N K_2HPO_4 buffer solution (pH 7.4) at 37 °C for 72 h.

A product ion scan of the protonated molecular ions of **4** and **5** (*m*/*z* = 430) showed a fragment at *m*/*z* = 314, which corresponds to the loss of a 2-deoxyribose moiety. The UV spectrum of **4** showed an absorption maximum (λ_{max}) at 259 nm (pH 7), which is consistent with *N*1-(3-chloro-2-hydroxy-3-buten-1-yl)-2′-deoxyadenosine obtained from the reaction of 1-chloroethenyl oxirane with 2′-deoxyadenosine.[17] Further characterization was carried out in [D_6]DMSO with 2D NMR spectroscopy.

The HMBC spectrum of **4** showed that 1′-H on 2-deoxyribose appeared as a triplet at 6.33 ppm, which correlated with three carbon signals (C-1′, C-4, and C-8, Figure 2). The correlation of 1′-H (6.33 ppm) with C-1′ (83.44 and 83.52 ppm) was confirmed by their mutual correlation in the HMQC spectrum (Figure S3, Supporting Information). The duplication of the carbon signals is due to the presence of two diastereomers. The second correlation of 1′-H with a quaternary carbon atom (147.15 and 147.10 ppm) could be assigned to C-4 on the adenine core. The third correlation of 1′-H with the methine carbon atom (C*H*) at 138.8 ppm was assigned to C-8 (see Figure 2, and Figure S1 in the Supporting Information). After confirming the C-8 peak, we assigned 8-H (8.34 ppm) from its correlation with C-8 in the HMBC and HMQC spectra (Figure S3). Although the HMBC spectrum of **4** did not show a correlation between 1′-H and the methylene C-2′, we assigned C-2′ from its correlation with 2′-H in the HMQC spectrum. Thus, the assignment of 2′-H was made through its correlation with 1′-H in the H,H-COSY spectrum (Figure S2). The peaks at 2.34 and 2.66 ppm were assigned to 2′′-H and 2′-H based on the coupling constants of $J_{2'3'}$ = 6.4 Hz (*trans*) and $J_{2''3'}$ = 3.2 Hz (*cis*) (Table 2) because the 2′-*endo* conformer of 2-deoxyribose is predominant in solution.[21,22] In the HMBC spectrum of **4**, C-4 was correlated with three protons at 6.33 (1′-H), 8.26 (2-H), and 8.34 ppm (8-H). The most downfield quaternary carbon signal at 156.0 ppm, which is coupled to 2-H but not 8-H, was assigned as C-6. The correlations of C-4 (147.15 and 147.10 ppm) and C-6 (156.0 ppm) with 2-H (8.34 ppm) and those of C-4 (147.15 and 147.10 ppm) and C-5 (123.6 ppm) with 8-H (8.26 ppm) were used to assign 2-H and 8-H. Additionally, α′-H and α′′-H were assigned to the signals at 2.63–2.70 and 2.74 ppm, respectively, by their correlations

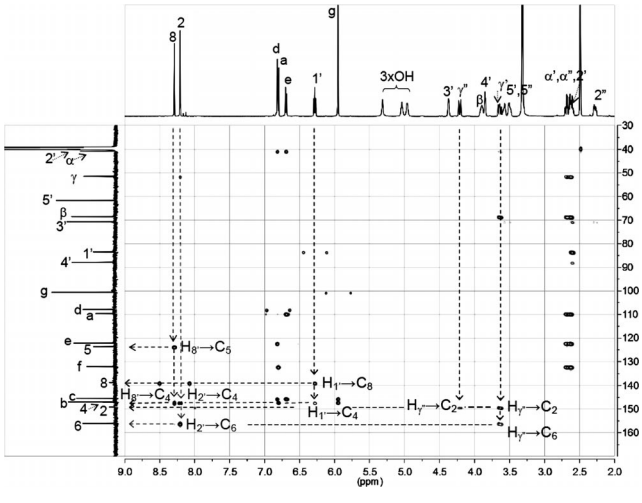

Figure 2. HMBC spectrum of **4** (500 MHz, [D_6]DMSO).

with C-a (109.6 ppm), C-e (122.2 ppm), and C-f (132.13 and 132.11 ppm) of the 1,3-benzodioxole group of **4** from the HMBC spectrum. The peak at 3.90 ppm was correlated to α′-H and α′′-H in the H,H-COSY spectrum, therefore, it was assigned as β-H. Finally, the correlations between C-2 and C-6 with γ′-H and γ′′-H support that **4** is an *N*1 adduct of 2′-deoxyadenosine (Figure 2 and Table 2).

The λ_{max} of a series of alkyl-substituted N^6-adenosines are redshifted compared to those reported for *N*1-adenosines.[23] The adduct **5**, which has a λ_{max} of 271 nm, was assigned to N^6γ-SFO-dAdo, because it is redshifted by 12 nm compared to **4** (259 nm). Compound **5** was further confirmed as the N^6 adduct by 2D NMR analysis. The HMQC spectrum of **5** showed unexpected correlations of a proton signal at 8.39 ppm with two carbon peaks at 139.4 and 164.6 ppm (Figure S5). In addition, the ^{1}H NMR spectrum of adduct **5** showed a puzzling extra proton when the integration of all the protons was summed up. It was subsequently established that the pair of signals at $^{13}C\delta$ = 164.6 ppm and $^1H\delta$ = 8.39 ppm were derived from the residual signals of the buffer, $HCOO^-NH_4^+$, which overlapped with 8-H of **5** in the ^{1}H NMR spectrum. The β-H peak at 3.91–3.95 ppm was determined from its correlation with methine C-β (70.2 ppm) in the HMQC spectrum (see also the DEPT spectrum of **5** in Figure S4). As expected, β-H showed correlations with two neighboring methylene protons γ′,γ′′-H and α′,α′′-H (Figure 3). By analyzing the multiple correlations of C-a (109.7 ppm), C-e (122.1 ppm), and C-f (132.9 ppm) with protons in the HMBC spectrum (Figure S6 and Table S1), we assigned the signals at 2.58–2.63 and 2.73–2.80 ppm to α′-H and α′′-H (Table S1). γ′-H and γ′′-H were then assigned to the signals at around 3.46 ppm because they also coupled with β-H in the H,H-COSY spectrum. The correlations of γ′-H and γ′′-H with the broadened NH peak (7.59 ppm) in Figure 3 revealed that **5** was an N^6 adduct of 2′-deoxyadenosine. Although the HMBC spectrum of **5** did not show a correlation between C-6 and γ′,γ′′-H, the chemical shifts of all of the carbons atoms on the adenine group are in excellent agreement with those of N^6-(3-chloro-2-hydroxy-3-buten-1-yl)-2′-deoxyadenosine.[17]

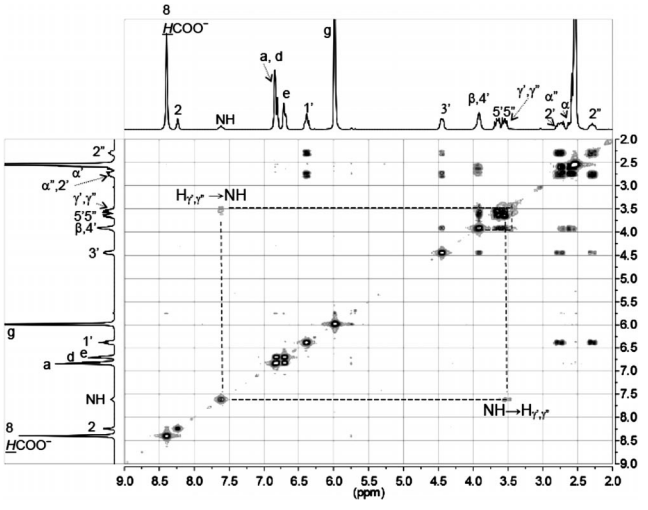

Figure 3. H,H-COSY spectrum of **5** (300 MHz, [D$_6$]DMSO).

We did not observe any ring opening adducts from the β attack of **2** or deamination of **4** to form an *N*1-inosine adduct, which has been reported in the reaction of styrene oxide with 2′-deoxyadenosine.[23–25] The lack of a phenyl or vinyl group on the α-carbon atom of an oxiran to stabilize the carbocation intermediate of an S_N1 reaction of **2** explains why no β attack and only γ attack adducts were observed; furthermore, the γ-position of **2** is sterically less hindered than the β-position. The secondary hydroxy group on the β-carbon atom of **4** cannot form an oxazolinium ring to facilitate the deamination process, therefore, the deamination product of **4** was not observed.[26]

Several carbon signals of 1:1 intensity ratios were observed in the NMR spectra of **4** due to the formation of diastereomers in the reaction of **3** with racemic **2**. In order to differentiate the diastereomeric pair of **4**, we intended to synthesize optically pure (*R*)-(+)-enriched **2** (Scheme 1) to react with **3**. However, a mixture of (*R*)/(*S*)-**2** (2:1 ratio) enriched with the (*R*)-(+)-form was obtained. The reaction produced similar adducts of **4** and **5** and their structures were identified as described above. The spectrum of (*R*)-enriched **4** showed that some of the ^{13}C NMR signals appeared to be in 2:1 ratios (Figure S8). However, ^{13}C NMR spectra of the diastereomers of **5** and (*R*)-(+)-enriched **5** did not show separate sets of peaks for the diastereomeric pairs (Figure S8). The diastereomeric pairs of **4** were further separated and collected by chiral HPLC (Figure S10). The peak area ratios of diastereomeric **4** and (*R*)-(+)-enriched **4** were 1:1 and 2:1, respectively, which were consistent with the peak area ratios observed in some of the ^{13}C NMR peaks. However, the diastereomeric pairs of **5** could not be separated under the same HPLC conditions.

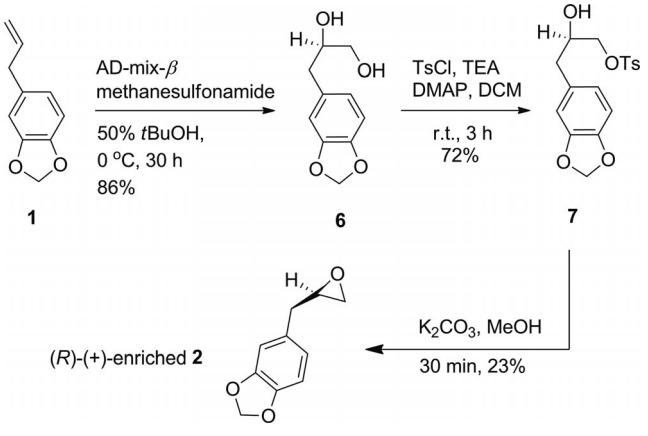

Scheme 1. Enantioselective synthesis of (*R*)-(+)-enriched **2**.

Rearrangement of 4 to 5

The *N*1 adduct of **3** usually undergoes Dimroth rearrangement to produce the N^6 adduct.[17,23–25] The transformation of **4** (an *N*1 adduct) to **5** (an N^6 adduct) by

Dimroth rearrangement was monitored with a reverse-phase HPLC system, which showed that **4** had a half life of ca. 24 h in K_2HPO_4 buffer solution at 37 °C.

Reaction of 2 with 8

The reaction of **2** with **8** was monitored by HPLC, which showed the formation of two products: **9** and **10** at t_R = 18.6 and 22.7 min, respectively (Figure 1b). The reaction of **2** with **8** at pH 7.4 at 37 °C for 72 h gave **9** and **10** in 1.0 and 2.4% isolated yields, respectively (Scheme 2). These two regioisomeric products had identical MS/MS fragmentation patterns (m/z = 314→136) but distinctive λ_{max} values in their UV spectra [λ_{max} = 274 (**9**), 263 nm (**10**), Table 1]. Further structural characterization of these two adducts was based on 2D NMR spectroscopy.

Table 1. UV λ_{max} of the DNA adducts of **2** at different pH values.

Adduct	λ_{max} [nm]		
	pH 1	pH 7	pH 13
4	259	259	261
5	267	271	271
9	274	274	273
10	260	263	263

The ^{1}H NMR spectrum of **9** showed two purine signals at 8.01 and 7.86 ppm. As 2-H in adenine adducts is normally downfield shifted compared to 8-H, the signal at 8.01 ppm was assigned to 2-H and that at 7.86 ppm was assigned to 8-H.[27,28] The ^{13}C NMR signals of C-2 (143.3 ppm) and C-8 (152.3 ppm) were then assigned based on the HMQC and DEPT spectra (Figures S13 and S11). The quaternary carbon signal at 118.9 ppm was assigned to C-5 of adenine based on its strong coupling with 8-H ($^3J_{CH}$) and weak coupling with 2-H ($^4J_{CH}$) in the HMBC spectrum of **9** (Figure 4). By comparing the chemical shifts of the adenine moiety in **9** with those in 3-(2-hydroxy-2-phenylethyl)adenine, which is derived from styrene oxide,[28] we assigned the signal at 148.2 ppm to C-4 and that at 156.7 ppm to C-6 (Table S2). The assignment of C-4 to the signal at 148.2 ppm was ascertained by its strong coupling with 2-H ($^3J_{CH}$) and weak couplings with γ′-H and γ′′-H ($^3J_{CH}$), and the assignment of C-6 (156.7 ppm) was ascertained by its correlations with 2-H ($^3J_{CH}$) and 8-H ($^4J_{CH}$) in the HMBC spectrum. The absence of a correlation between 8-H and C-4 ($^3J_{CH}$) and the presence of correlations between 2-H and C-5 and between 8-H and C-6 (both $^4J_{CH}$ couplings) in HMBC is unusual and could be due to the particular hybridization of these carbon atoms or other factors.[29] Based on the multiple couplings of C-a, C-e, and C-f in the HMBC spectrum of **9**, the proton signals at 2.58–2.60 and 2.89 ppm were assigned as α′-H and α′′-H. The methylene proton signals at 3.99–4.03 and 4.35 ppm were subsequently assigned as γ′-H and γ′′-H based on DEPT, HMQC, and H,H-COSY spectra (Figure S12). Finally, the

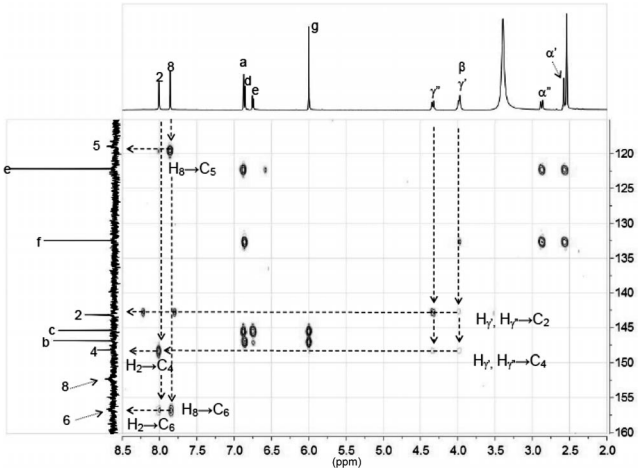

Figure 4. HMBC spectrum of **9** (500 MHz, in [D$_6$]DMSO).

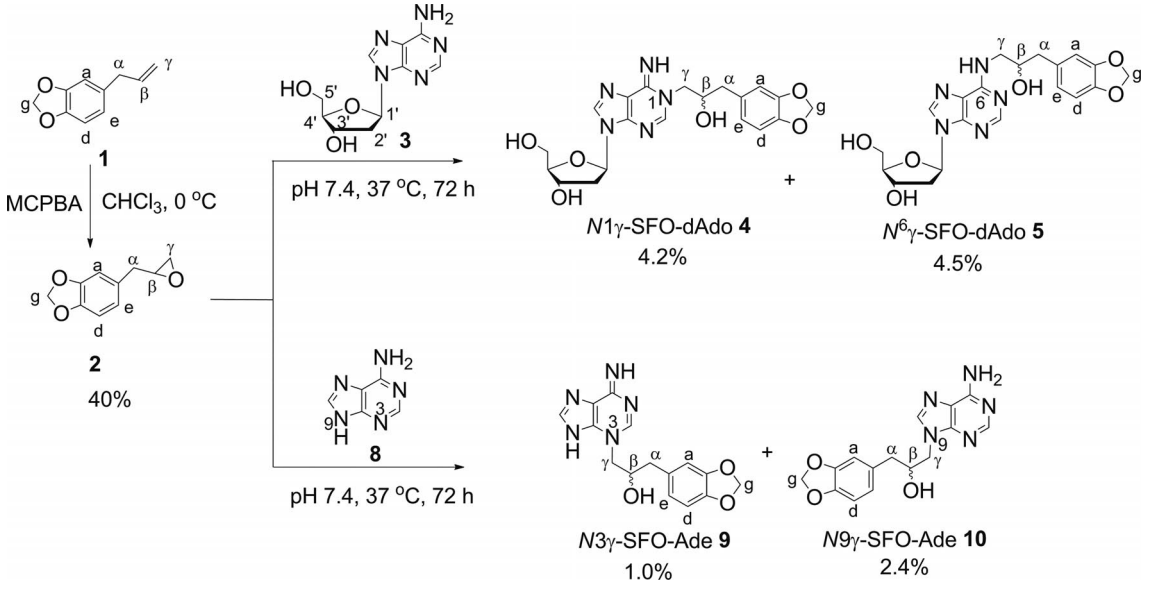

Scheme 2. Syntheses of **4**, **5**, **9**, and **10**.

correlations of γ′-H and γ′′-H with C-2 and C-4 indicated that **9** is consistent with an *N*3 adduct of adenine (Figure 4 and Table S2).

The proton signals of the purine ring of **10** were observed at 8.10, 8.02, and 7.12 ppm and were assigned to 2-H, 8-H, and NH_2, respectively. Based on the proton assignments of adenine, the carbon signal at 141.5 ppm coupled to 8-H was assigned as C-8 from the HMQC and DEPT spectra (Figures S16 and S14). The carbon signal at 118.5 ppm in the HMBC spectrum (Figure 5) was assigned to C-5 because it was connected to both 8-H ($^3J_{CH}$) and NH_2 ($^3J_{CH}$). Similarly, the carbon signal at 149.6 ppm, which was coupled to both 2-H ($^3J_{CH}$) and 8-H ($^3J_{CH}$), was assigned to C-4. In addition, the carbon signal at 155.8 ppm was assigned to C-6 because it was coupled to 2-H ($^3J_{CH}$) but not to 8-H ($^4J_{CH}$). The assignment of γ′-H and γ′′-H (3.98 and 4.15 ppm, respectively) was determined by DEPT, HMQC, HMBC, and H,H-COSY spectra (Figure S15) as depicted in Figure 5. The correlations of the methylene protons γ′-H and γ′′-H with C-8 and C-4 supported that **10** arose from the reaction of *N*9-adenine on the γ-position of **2** (Figure 5 and Table S3).

The methine carbons of the adenine unit that are closer to the alkyl substituents are upfield shifted; for example, C-2 of **9** (an *N*3 adduct) was at 143.3 ppm, whereas that of C-8 was at 152.3 ppm. Similarly, C-8 of **10** (an *N*9 adduct) was at 141.5 ppm, whereas that of C-2 was at 152.2 ppm. These observations are consistent with those reported by Linhart et al. in their ^{13}C NMR assignments of *N*3-(2-hydroxy-2-phenylethyl)adenine and *N*9-(2-hydroxy-2-phenylethyl)adenine.[27] The *N*3 position of **8** is not involved in Watson–Crick hydrogen bonding and is exposed in the minor groove of DNA, which is therefore susceptible to alkylation.[30] In order to obtain a large amount of the *N*3 adduct, we used **8** to react with **2**. The reaction of **2** with **8** provided **9** and **10**. However, **10** is not expected to form in the reaction of **2** with DNA. Hence, we used **10** as internal standard to quantify the formation of **9** in **2**-pretreated calf thymus DNA.

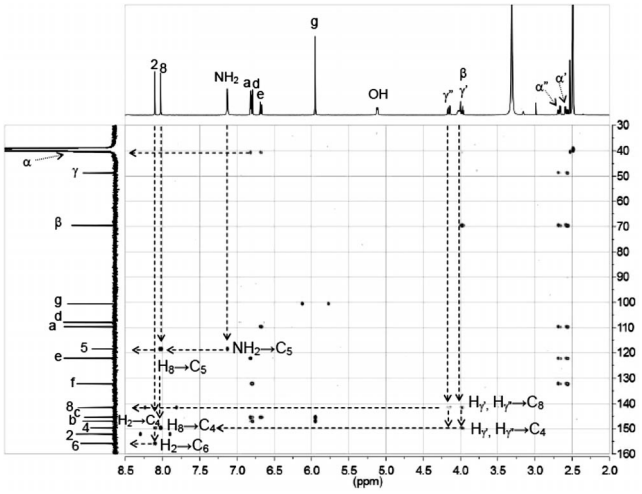

Figure 5. HMBC spectrum of **10** (500 MHz, in [D_6]DMSO).

Reaction of 2 with Calf Thymus DNA

The products of the reaction of **2** with calf thymus DNA were analyzed by HPLC–ESI-MS/MS in the multiple reaction monitoring (MRM) mode, and the *m*/*z* signals at 430→314 for **4** and **5**, 435→319 for [$^{15}N_5$]-**4** and [$^{15}N_5$]-**5**, and 314→136 for **9** and **10** were used for this purpose. The DNA adducts were identified by comparison of their retention times with those of the corresponding authentic samples. In the incubation solution, only **9** was measured (Figure 6, a), which suggested that **9** was easily depurinated from the DNA backbone, and reached a level of 400 per 10^6 nucleotides. In the enzymatic DNA hydrolysate, the levels of **4** and **5** were calculated to be 2000 and 170 per 10^6 nucleotides, respectively, and that of **9** reached 660 per 10^6 nucleotides (Figure 6, b). Furthermore, the formation of adducts **4**, **5**, and **9** in double stranded DNA were traced at different time intervals. The initial level of **9** was higher than those of **4** and **5** (0–10 h) and reached a plateau at 24 h. The formation of **4** was accompanied by a tiny amount of **5**,

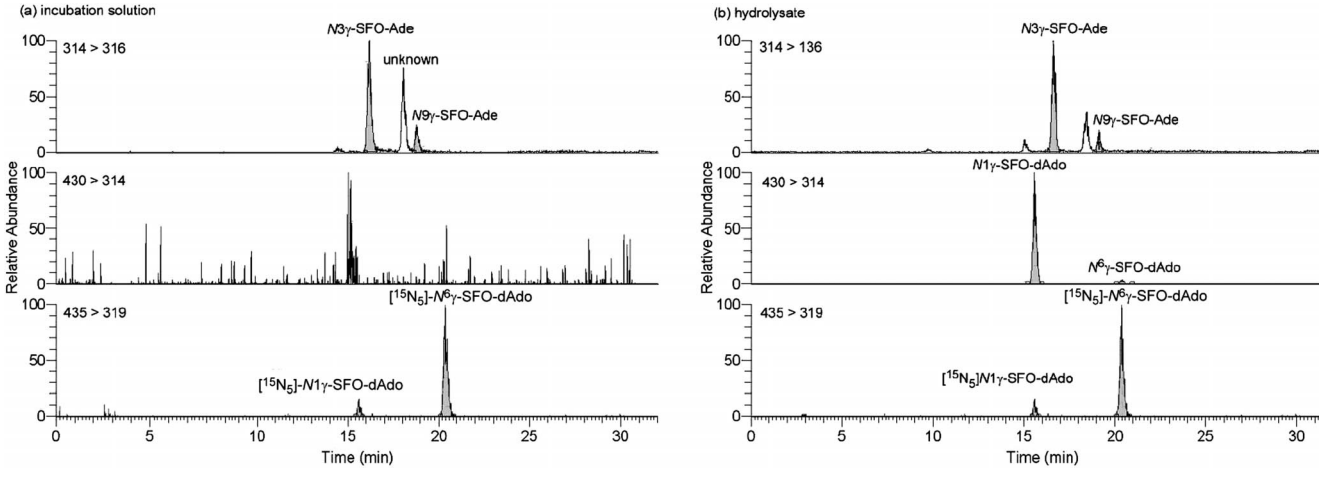

Figure 6. HPLC–ESI-MS/MS of **2**-pretreated calf thymus DNA (a) incubation solution and (b) hydrolysate of enzymatic hydrolysis.

which demonstrated that *N*1 was the initial reaction site and the *N*1 adduct **4** was slowly converted to the N^6 adduct **5** by the Dimroth rearrangement (Figure S17).

Styrene oxide (SO), which is structurally similar to **2**, has been proven to contribute to gene mutation.[31] We therefore speculated that **2** may have a similar biological relevance to SO. For example, *N*1- and N^6-adenine adducts of SO, which resulted in AT→GC transitions, have been reported.[32,33] *N*1-adenine adducts may contribute more to the mutation of AT-base pairs because their central hydrogen bonds are blocked. *N*3-Adenine adducts are prone to depurination from the DNA backbone and DNA polymerase preferentially adds an adenine opposite to an apurinic site,[32] therefore, they tend to lead to AT→TA transversions. Such a mutation has been observed in SO-treated hypoxanthine–guanine phosphoribosyl transferase mutant clones of primary human T-lymphocytes.[34]

Conclusions

We have purified the reaction products of (±)-SFO (**2**) with 2′-deoxyadenosine (**3**) and adenine (**8**) and determined their structures by UV, 1D and 2D NMR spectroscopy and MS. The reaction of **2** with **3** gave **4** and **5** in 4.2–4.5% yield, and that of **2** with **8** gave **9** and **10** in 1.0–2.4% yield. These adducts were also detected in **2**-pretreated calf thymus DNA and were accurately quantified by our newly-developed HPLC–ESI-MS/MS method. This is the first systematic characterization of the adducts formed from the reactions of **2** with **8** and **3**, and the results suggest that further in vitro and in vivo studies are needed to shed light on the carcinogenicity of **2**.

Experimental Section

Chemicals and Enzymes: Compounds **3** and **8**, calf thymus DNA, deoxyribonuclease I from bovine pancreas type IV, posphodiesterase II from bovine spleen, posphodiesterase I from Crotalus atrox type IV, and acid phosphatase from potato were purchased from Sigma–Aldrich Company Ltd (St Louis, MO). [$^{15}N_5$]-2′-deoxyadenosine was purchased from Medical Isotope Inc. (Pelham, NH). HPLC grade acetonitrile was purchased from Mallinkrodt Baker Inc. (Paris, KY). Ammonium formate was obtained from Fluka Biochemika (Steinheim, Germany). Formic acid was purchased from Riedel-de Haën (Seelze, Germany). Water was purified with a Milli-RO/Milli-Q system (Millipore, Bedford, MA). Compound **2** was prepared according to a literature procedure.[35]

Purification of DNA Adducts: Reverse-phase HPLC was performed with a Hitachi L-7000 pump system with a D-7000 interface, L-7200 autosampler (Hitachi Ltd., Tokyo), column oven, L-7450A photodiode array detector (Hitachi Ltd., Tokyo), and a Prodigy ODS (3) column, 4.6× 250 mm, 5 μm (Phenomenex, Torrance, CA). Ammonium formate buffer (pH 5.5, 50 mM) in acetonitrile (58:42, v/v) was used as the mobile phase to separate the reaction mixtures of **3** and **8** with **2**. The temperature of the column oven was set at 25 °C. Chiral HPLC was performed with a Gilson 321-H1 pump system with a 506C interface, a Rheodyne 7725I injector, a Gilson 155 UV/Vis detector, Gilson Unipoint software (Gilson, Inc., Middleton, WI), and CHIRALPAK AS-H column, 4.6× 250 mm, 5 μm (Daicel Chemical Industrial Ltd., Tokyo). The mobile phase of 2-propanol/hexane (20:80, v/v) was eluted isocratically at a flow rate of 0.5 mL/min to purify **6**, **7**, and (*R*)-(+)-enriched **2**. Compounds **4** and **5** were eluted with 2-propanol/hexane (2:98, v/v) at a flow rate of 0.5 mL/min for 5 min, and then with 2-propanol/hexane (90:10, v/v) solution with the flow rate decreased to 0.1 mL/min from 5 to 6 min and maintained for 90 min.

Spectroscopic and Spectrometric Methods: ^{1}H NMR spectra were measured with a 300 or 500 MHz spectrometer. Natural abundance ^{13}C NMR spectra were recorded using pulse Fourier transform techniques with a 300 or 500 MHz NMR spectrometer operating at 75.4 or 125.7 MHz, respectively. Broadband decoupling, H,H-COSY, HMQC, and HMBC were carried out to simplify spectra and aid peak identification. Samples were dissolved in [D_6]DMSO for NMR analysis. The alkylation positions of the DNA adducts were mainly determined by long-range H–C correlations in the HMBC spectra. UV/Vis spectra of the adducts at pH 1, 7, and 13 were recorded with a HP-8453 spectrophotometer with diode array detection. HPLC–ESI-MS/MS was performed on an API 3000TM spectrometer (Applied Biosystems/MDS SCIEX, Foster City, CA) together with Hitachi L-7000 pump and L-7200 autosampler (Hitachi Ltd., Tokyo). An electrospray ionization source was used in the positive mode (ESI-MS/MS). A Prodigy ODS (3) column, 2.1×150 mm, 5 μm (Phenomenex, Torrance, CA) was used. Total ion chromatograms and mass spectra were recorded on a personal computer with the Analyst software version 1.1 (Applied Biosystems). The pure compounds were diluted with a 1:1 (v/v) mixture of 0.1% formic acid and pure acetonitrile followed by introducing them into the ion source with a syringe pump at a flow rate of 5 μL/min to characterize their structure. The mobile phase consisted of a linear gradient from 0 to 42% acetonitrile in 50 mM ammonium formate buffer (pH 5.5) from 0 to 25 min at a flow rate of 200 μL/min. The MRM mode was used for quantitative analysis of **4** and **5** (*m*/*z* = 430→314), [$^{15}N_5$]-**4** and [$^{15}N_5$]-**5** (*m*/*z* = 435→319), and **9** and **10** (*m*/*z* = 314→136) with the collision energy set at 29, 27, 35, and 39 V, respectively. The dwell time for MRM experiments was set at 150 ms. Nitrogen was used as the turbo gas with temperature set at 450 °C; it was also used as the nebulizer, curtain, and collision gas with pressure settings of 8, 8, and 12 psi, respectively. Calibration curves were established in the concentration range of 5 to 250 ng/mL for **4**, **5**, and **9**.

Synthesis of (±)-SFO (2):[35] *m*-Chloroperbenzoic acid (30 g, 0.17 mol) in chloroform (200 mL) was added slowly to a solution of safrole (**1**, 22.7 mL, 0.15 mol) in chloroform (50 mL) at 0 °C. The reaction mixture was stirred at room temperature overnight, and the excess *m*-chloroperbenzoic acid was treated with 10% sodium sulfite. After extraction into 5% $NaHCO_3$ (3× 250 mL) and washing with water (2× 200 mL), the organic layers were combined and dried with $MgSO_4$ before the solvents were evaporated to dryness. The residue was purified by column chromatography with hexane/EtOAc (10:1, v/v) as the eluent to give **2** as a yellow liquid (10.6 g, 40%). ESI-MS: *m*/*z* = 179 [M + H]$^+$. ^{1}H NMR (300 MHz, $CDCl_3$): δ = 2.51 (dd, J_1 = 2.6, J_2 = 4.9 Hz, 1 H, γ′-H), 2.70–2.81 (m, 3 H, γ′′-H, α′-H, α′′-H), 3.06–3.11 (m, 1 H, β-H), 5.91 (s, 2 H, g-H), 6.66–6.69 (m, 1 H, Ar-C*H*), 6.73–6.75 (m, 2 H, Ar-C*H*) ppm. ^{13}C NMR (75.4 MHz, $CDCl_3$): δ = 38.3 (C-γ), 46.7 (C-α), 52.5 (C-β), 100.8 (C-g), 108.2 (C-d), 109.4 (C-a), 122.8 (C-e), 130.7 (C-f), 146.2 (C-c), 147.6 (C-b) ppm.

Enantioselective Synthesis of (*R*)-(+)-Enriched 2[36]

(*R*)-(+)-5-(2,3-Dihydroxypropyl)-1,3-benzodioxole (6): A mixture of **1** (0.16 mL, 1.0 mmol), AD-mix-β (1.4 g, 0.1 mmol), and methanesulfonamide (98 mg, 1.0 mmol) in 50% aqueous *t*BuOH (10 mL)

was stirred at 0 °C for 30 h. Na_2SO_3 (1.5 g) was added and the mixture was extracted into EtOAc (3 × 10 mL). The organic layer was washed with brine, dried with $MgSO_4$, and evaporated under reduced pressure on a rotary evaporator. The residue was recrystallized from CH_2Cl_2 to give **6** as a white solid (86%). Compound **6** showed 96% *ee*, determined by Chiral HPLC (Figure S7). The optical rotation of **6**, $[\alpha]_D^{25}$ = +21.7 (*c* = 0.003, CH_2Cl_2), was different to the literature value ($[\alpha]_D$ = +32).[36] ^{1}H NMR (300 MHz, $CDCl_3$): δ = 2.61–2.74 (m, 2 H, α-H), 3.49 (dd, J_1 = 7.0, J_2 = –11.2 Hz, 1 H, γ′-H), 3.67 (dd, J_1 = 3.2, J_2 = –11.2 Hz, 1 H, γ′′-H), 3.83–3.91 (m, 1 H, β-H), 5.93 (s, 2 H, g-H), 6.66 (dd, J_1 = 1.6, J_2 = 7.9 Hz, 1 H, e-H), 6.72 (d, *J* = 1.6 Hz, 1 H, a-H), 6.75 (d, *J* = 7.9 Hz, 1 H, d-H) ppm. ^{13}C NMR (75.4 MHz, $CDCl_3$): δ = 39.4 (C-α), 65.9 (C-γ), 73.0 (C-β), 100.9 (C-g), 108.3 (C-d), 109.6 (C-a), 122.2 (C-e), 131.3 (C-f), 146.3 (C-c), 147.8 (C-b) ppm.

(*R*)-(+)- 5-(2-Hydroxy-3-tosyloxypropyl)-1,3-benzodioxole (7): To a mixture of **6** (0.42 g, 2.14 mmol), tosyl chloride (0.45 g, 2.35 mmol), and 4-dimethylaminopyridine (0.03 g, 0.24 mmol) in CH_2Cl_2 (7 mL) was added triethylamine (0.36 mL) in CH_2Cl_2 (7 mL) dropwise at 0 °C, and the mixture was stirred at room temperature for 3 h. The residue was purified by column chromatography (hexane/EtOAc = 75:25, R_f = 0.12) to give **7** as a light yellow liquid (72%). Compound **7** was determined to have 40% *ee* by chiral HPLC analysis (Figure S7). $[\alpha]_D^{25}$ = +12.5 (*c* = 0.002, CH_2Cl_2). ^{1}H NMR (300 MHz, $CDCl_3$): δ = 2.46 (s, 3 H, C*H*$_3$), 2.67–2.71 (m, 2 H, α-H), 3.90–4.06 (m, 3 H, β-H, γ′-H, γ′′-H), 5.93 (s, 2 H, f-H), 6.59 (dd, J_1 = 1.6, J_2 = 7.9 Hz, 1 H, e-H), 6.63 (d, *J* = 1.5 Hz, 1 H, a-H), 6.72 (d, *J* = 7.9 Hz, 1 H, d-H), 7.34 (d, *J* = 8.1 Hz, 2 H, Ar-C*H*), 7.80 (d, *J* = 8.3 Hz, 2 H, Ar-C*H*) ppm. ^{13}C NMR (75.4 MHz, $CDCl_3$): δ = 21.6 (C*H*$_3$), 38.9 (C-α), 70.3 (C-β), 72.5 (C-γ), 100.9 (C-g), 108.3 (C-d), 109.5 (C-a), 122.2 (C-e), 127.9 (*C*HCSO$_3$), 129.9 (CH$_3$C*C*H), 130.2 (C-f), 132.5 (CH$_3$*C*CH), 145.1 (CH*C*SO$_3$),146.3 (C-c), 147.7 (C-b) ppm.

Synthesis of (*R*)-(+)-5-Oxiranylmethyl-1,3-benzodioxole (2): A mixture of **7** (0.13 g, 0.40 mmol) and K_2CO_3 (0.49 g, 3.57 mmol) in methanol (25 mL) was stirred at room temperature for 30 min. The methanol was removed with a rotary evaporator. The residue was diluted with water and extracted into EtOAc. The organic layer was dried with $MgSO_4$ and the solvent was removed with a rotary evaporator. The crude product was purified by column chromatography (hexane/EtOAc = 7:3, R_f = 0.58) to give **2** as a light yellow liquid (23%). Compound **2** was determined to have 39% *ee* by chiral HPLC analysis (Figure S7). The separated enantiomers were collected for optical rotation measurements. (*R*)-(+)-5-Oxiranylmethyl-1,3-benzodioxole **2**: $[\alpha]_D^{25}$ = +11.8 (*c* = 0.003, CH_2Cl_2); (*S*)-(–)-5-Oxiranylmethyl-1,3-benzodioxole **2**: $[\alpha]_D^{25}$ = –11.6 (*c* = 0.003, CH_2Cl_2). $[\alpha]_D^{25}$ = +13 has been reported for the (*R*)-(+) enantiomer.[36] ^{1}H NMR (300 MHz, $CDCl_3$): δ = 2.47 (dd, J_1 = 2.6, J_2 = 4.9 Hz, 1 H, γ′-H), 2.65–2.79 (m, 3 H, γ′′-H, α′, α′′-H), 3.01–3.07 (m, 1 H, β-H), 5.87 (s, 2 H, CH_2), 6.60–6.64 (m, 1 H, Ar-C*H*), 6.68 (s, 1 H, Ar-C*H*), 6.95 (d, *J* = 6.1 Hz, 1 H, Ar-C*H*) ppm. ^{13}C NMR (75.4 MHz, in $CDCl_3$): δ = 38.4 (C-γ), 46.8 (C-α), 52.5 (C-β), 100.9 (C-g), 108.3 (C-d), 109.5 (C-a), 121.9 (C-e), 130.8 (C-f), 146.5 (C-c), 147.7 (C-b) ppm.

Synthesis of N^1γ-SFO-dAdo (4), (*R*)-Enriched 4, N^6γ-SFO-dAdo (5), and (*R*)-Enriched 5: A solution of **2** or (*R*)-(+)-enriched **2** was treated with **3** in a 2:1 molar ratio in 0.2 N K_2HPO_4 (pH 7.4) solution and incubated at 37 °C for 72 h. The products were purified and desalted using reverse-phase HPLC. Solutions of the pure adducts were dried under vacuum. Each pure adduct was subjected to spectroscopic and spectrometric characterization. The characteristic UV λ_{max} of **4** and **5** at different pH values are presented in Table 1. The ESI-MS/MS of **4** and **5** showed the same fragments at *m*/*z* = 430 $[M + H]^+$, 452 $[M + Na]^+$, and 314 [M – 2-deoxyribose + $H]^+$. HRMS (ESI) for **4**: calcd. for $C_{20}H_{24}N_5O_6$ $[M + H]^+$ 430.1728; found 430.1729. HRMS (ESI) for **5**: calcd. for $C_{20}H_{24}N_5O_6$ $[M + H]^+$ 430.1728; found 430.1723. The ^{1}H and ^{13}C NMR spectroscopic data for **4** and **5** are presented in Tables 2 and S1, respectively.

(*R*)-Enriched 4: ^{1}H NMR (500 MHz, [D$_6$]DMSO): δ = 2.29–2.37 (m, 1 H, 2′′-H), 2.62–2.78 (m, 3 H, 2′-H, α′, α′′-H), 3.51–3.73 (m, 3 H, 5′, 5′′-H, γ′-H), 3.87–3.91 (m, 2 H, 4′-H, β-H), 4.24–4.29 (m, 1 H, γ′′-H), 4.41–4.43 (m, 1 H, 3′-H), 6.00 (s, 2 H, g-H), 6.31–6.36 (m, 1 H, 1′-H), 6.75 (dd, J_1 = 1.6, J_2 = 7.9 Hz, 1 H, e-H), 6.86 (d, *J* = 7.9 Hz, 1 H, d-H), 6.87 (s, 1 H, a-H), 8.26 (s, 1 H, 2-H), 8.35 (s, 1 H, 8-H) ppm. ^{13}C NMR (125.7 MHz, [D$_6$]DMSO): δ = 40.7 (C-α), 51.4 (C-γ), 61.6 (C-5′), 68.5 (C-β), 70.6 (C-3′), 83.41 and 83.48 (C-1′) overlapped with solvent (C-2′), 87.9 (C-4′), 100.6 (C-g), 107.9 (C-d), 109.6 (C-a), 122.1 (C-e), 123.6 (C-5), 132.09 and 132.11 (C-f), 138.74 and 138.79 (C-8), 145.4 (C-c), 146.9 (C-b), 147.07 and 147.12 (C-4), 149.2 (C-2), 156.0 (C-6) ppm.

(*R*)-Enriched 5: ^{1}H NMR (500 MHz, [D$_6$]DMSO): δ = 2.30 (ddd, $J_{2''3'}$ = 2.9, $J_{1'2''}$ = 6.1, $J_{2'2''}$ = –13.1 Hz, 1 H, 2′′-H), 2.60–2.63 (m, 1 H, α′-H), 2.72–2.79 (m, 2 H, 2′-H, α′′-H), 3.54 (br. s, γ′, γ′′-H ovrelap with H_2O), 3.54–3.57 (m, 1 H, 5′′-H), 3.66 (dd, $J_{4'5'}$ = 3.4, $J_{5'5''}$ = –11.7 Hz, 1 H, 5′-H), 3.91–3.93 (m, 2 H, 4′-H, β-H), 4.44–4.45 (m, 1 H, 3′-H), 5.03 (br. s, 1 H, OH), 5.28 (br. s, 1 H, OH), 5.37 (br. s, 1 H, OH), 5.98 (s, 2 H, g-H), 6.38 (dd, $J_{1'2''}$ = 6.2, $J_{1'2'}$ = 7.7 Hz, 1 H, 1′-H), 6.70 (d, *J* = 7.9 Hz, 1 H, e-H), 6.82 (d, *J* = 7.9 Hz, 1 H, d-H), 6.84 (s, 1 H, a-H), 7.59 (br. s, 1 H, NH-6), 8.23 (s, 1 H, 2-H), 8.38 (s, 1 H, 8-H) ppm. ^{13}C NMR (125.7 MHz, [D$_6$]DMSO): δ = 40.7 (C-α), 46.0 (C-γ), 61.9 (C-5′), 70.3 (C-β), 71.0 (C-3′), 84.0 (C-1′) overlapped with solvent (C-2′), 88.0 (C-4′), 100.6 (C-g), 107.9 (C-d), 109.8 (C-a), 119.7 (C-5), 122.2 (C-e), 133.0 (C-f), 139.5 (C-8), 145.3 (C-c), 146.9 (C-b), 148.1 (C-4), 152.3 (C-2), 154.6 (C-6) ppm.

Synthesis of [$^{15}N_5$]-4 and [$^{15}N_5$]-5: [$^{15}N_5$]-2′-deoxyadenosine (5 mg) was dissolved in H_2O (1 mL) to serve as the stock solution. Compound **2** (20 μmol) was added to [$^{15}N_5$]-2′-deoxyadenosine (500 μL, 10 μmol) in 0.2 N K_2HPO_4 (pH 7.4) buffer solution, and the mixture was incubated at 37 °C for 72 h. The reaction mixture was subjected to HPLC separation as mentioned above. The corresponding peaks were collected.

Synthesis of N^3γ-SFO-Ade (9) and N^9γ-SFO-Ade (10): A mixture of **2** and **8** in a 2:1 molar ratio in 0.2 N K_2HPO_4 (pH 7.4) buffer solution was incubated at 37 °C for 72 h. The adducts were purified and desalted using reverse-phase HPLC. The pure adduct was dried under vacuum and subjected to spectroscopic and spectrometric characterization. The characteristic λ_{max} of **9** and **10** at different pH values are presented in Table 1. The ESI-MS/MS of **9** and **10** showed the same fragments at *m*/*z* = 314 $[M + H]^+$ and 136 [M – SFO + $H]^+$. HRMS (ESI) for **9**: calcd. for $C_{15}H_{16}N_5O_3$ $[M + H]^+$ 314.1255; found 314.1243. HRMS (ESI) for **10**: calcd. for $C_{15}H_{16}N_5O_3$ $[M + H]^+$ 314.1255; found 314.1242. The ^{1}H and ^{13}C NMR spectroscopic data for **9** and **10** are presented in Tables S2 and S3, respectively.

Rearrangement of 4 to N^6γ-SFO-dAdo (5): A sample of **4** (30 μg) in 0.2 N K_2HPO_4 (1 mL, pH 7.4) solution was incubated at 37 °C, and the solution was analyzed at various time intervals by reverse-phase HPLC.

Reaction of 2 with Calf Thymus DNA: Calf thymus DNA (1 mg) in Tris-HCl buffer (pH 7.5–8.5, 1 mL), which contained 1 mM ethylenediaminetetraacetic acid, was stored at 4 °C overnight to serve

Table 2. ^{1}H and ^{13}C NMR chemical shifts (δ), coupling constants ($J_{H,H}$), and HMBC correlations for **4**.

Proton[a]	δ [ppm]	Multiplicity	$J_{H,H}$ [Hz]	Carbon	δ [ppm][a] (*R*)/(*S*) = 1:1	δ [ppm][a] (*R*)/(*S*) = 2:1	HMBC correlation(s)
2-H	8.26	s		C-2	149.2	149.2	2-H; γ-H
8-H	8.34	s		C-8[e]	138.8	138.74; 138.79	1′-H; 8-H
6-NH	n.d.[c]			C-6	156.0	156.0	2-H; γ-H
				C-4[e]	147.15; 147.10	147.12; 147.07	1′-H; 8-H
				C-5	123.6	123.6	8-H
1′-H	6.33	t	$J_{1'2'}$ = 7.2[f] $J_{1'2''}$ = 6.4[f]	C-1′[e]	83.44; 83.52	83.41; 83.48	2′-H; 1′-H
2′′-H	2.31–2.36	ddd	$J_{1'2''}$ = 6.4[g] $J_{2'2''}$ = –12.8[g] $J_{2''3'}$ = 3.2[g]	C-2′	–	–	
2′-H	2.63–2.70[d]	m	$J_{1'2'}$ = 7.2[g] $J_{2'2''}$ = –12.8[g] $J_{2'3'}$ = 6.4[g]				
3′-H	4.42	br. s		C-3′[e]	70.67; 70.65	70.6	2′-H; 5′-H
4′-H	3.90	br. s[b]		C-4′[e]	87.92; 87.94	87.9	2′-H
5′′-H	3.53–3.56	m[b]		C-5′	61.6	61.6	
5′-H	3.61–3.64	m[b]					
3′-OH	5.37	br. s					
5′-OH	5.08–5.10	m[b]					
β-OH	5.01	d	4.4				
α-H	2.63–2.70[d]	m		C-α	40.7	40.7	e-H; d-H
	2.74	dd	5.0; –14.0				
β-H	3.90	br. s[b]		C-β	68.5	68.5	α-H; γ-H
γ-H	3.67, 3.72	m[b]		C-γ	51.4	51.4	2-H; α-H
	4.27	dd	2.4; –13.3				
a-H	6.87	d	1.2	C-a	109.6	109.6	α-H; e-H; d-H
				C-b	147.0	146.9	g-H; a-H
				C-c	145.4	145.4	g-H; e-H; a-H
d-H	6.86	d	7.9	C-d	107.9	107.9	d-H
e-H	6.74	dd	1.1; 7.9	C-e	122.2	122.1	α-H; e-H
				C-f[e]	132.13; 132.11	132.11; 132.09	α-H; e-H
g-H	6.00	s		C-g	100.6	100.6	g-H

[a] Diastereomeric mixture of racemic **4** or (*R*)-enriched **4**. [b] Unresolved multiplet due to a mixture of diastereomers. [c] n.d. = not detected. [d] The signals of 2′′-H and α-H were overlapped. [e] Separated shifts due to a mixture of diastereomers. [f] Selective decoupling of 2′-H or 2′′-H. [g] ^{1}H NMR spectra measured with an 800 MHz spectrometer.

as the stock solution. A solution of DNA (100 μL, 100 μg) was hydrolyzed with a mixture of DNase I (4 U), phosphodiesterase I (32 mU), phosphodiesterase II (80 mU), and acid phosphatase (1 U) and incubated at 37 °C for 8–10 h.[37,38] The amounts of reagents were adjusted according to the amount of DNA in the sample. To evaluate the efficiency of the enzymatic hydrolysis, calibration curves of dAdo, dGuo, dCyd, and dThd were established by HPLC analysis. The retention time of each 2′-deoxyribonucleoside was at 9.9 min (dCyd), 12.4 min (dGuo), 14.6 min (dThd), and 16.7 min (dAdo, data not shown), respectively. The hydrolysis efficiency of double strand calf thymus DNA was estimated to be 97.8%.

Calf thymus DNA (10 mg) was treated with **2** (60 μmol) in 0.2 N K_2HPO_4 buffer (10 mL, pH 7.4) and incubated at 37 °C for 72 h. Two samples (each 400 μL) were removed from the reaction mixture at different time intervals (0, 0.5, 2, 4, 6, 8, 10, 24, 48, and 72 h). The reaction mixture was extracted into Et_2O to remove unreacted **2**. All the samples were then kept in an ice bath for a few hours to vaporize the Et_2O and then analyzed using two different methods modified from Goggin et al.[39] Method 1: The solution was spiked with [$^{15}N_5$]-**4** (100 μL, 4 ng), [$^{15}N_5$]-**5** (100 μL, 9 ng), and **10** (5 ng) to serve as internal standards and then filtered through a 0.22 μm PVDF membrane to remove the DNA backbone for HPLC–ESI-MS/MS analysis. Method 2: The reaction mixture was subjected to hydrolysis of the biopolymer using the enzymatic method described above (final volume 1 mL), and analyzed after removal of the enzymes by filtration. The calibration curve of each DNA adduct with added internal standards was established for quantitative analysis by HPLC–ESI-MS/MS.

Supporting Information (see footnote on the first page of this article): DEPT, H,H-COSY, and HMQC spectra of **4**, **5**, **9**, and **10**, HMBC spectrum of **5**, chiral HPLC analysis of precursors to **2** and **4**, time-dependent analysis of all adducts by HPLC–ESI-MS/MS, NMR spectroscopic data of all adducts, and data for the formation of **4**, **5**, and **9** in calf thymus DNA.

Acknowledgments

This work was supported in part by the Environmental and Occupational Center grant from the National Taiwan University and National Science Council (project to WSC, NSC-99-2119-M-009-001-MY2). We also thank Prof. Chung-Ming Sun at NCTU for the specific rotation measurements.

[1] J. M. Lee, T. Y. Liu, D. C. Wu, H. C. Tang, J. Leh, M. T. Wu, H. H. Hsu, P. M. Huang, J. S. Chen, C. J. Lee, Y. C. Lee, *Mutat. Res.* **2005**, *565*, 121–128.
[2] H. Daimon, S. Sawada, S. Asakura, F. Sagami, *Carcinogenesis* **1998**, *19*, 141–146.
[3] D. H. Phillips, M. V. Reddy, K. Randerath, *Carcinogenesis* **1984**, *5*, 1623–1628.

[4] K. Randerath, R. E. Haglund, D. H. Phillips, M. V. Reddy, *Carcinogenesis* **1984**, *5*, 1613–1622.
[5] M. J. W. Chang, C. Y. Ko, R. F. Lin, L. L. Hsieh, *Arch. Environ. Contam. Toxicol.* **2002**, *43*, 432–437.
[6] C. L. Chen, C. W. Chi, K. W. Chang, T. Y. Liu, *Carcinogenesis* **1999**, *20*, 2331–2334.
[7] P. G. Wislocki, P. Borchert, J. A. Miller, E. C. Miller, *Cancer Res.* **1976**, *36*, 1686–1695.
[8] P. Borchert, J. A. Miller, E. C. Miller, T. K. Shires, *Cancer Res.* **1973**, *33*, 590–600.
[9] G. Luo, T. M. Guenthner, *Drug Metab. Dispos.* **1996**, *24*, 1020–1027.
[10] D. H. Phillips, J. A. Miller, E. C. Miller, B. Adams, *Cancer Res.* **1981**, *41*, 2664–2671.
[11] A. B. Swanson, D. D. Chambliss, J. C. Blomquist, E. C. Miller, J. A. Miller, *Mutat. Res.* **1979**, *60*, 143–153.
[12] P. G. Wislocki, E. C. Miller, J. A. Miller, E. C. McCoy, H. S. Rosenkranz, *Cancer Res.* **1977**, *37*, 1883–1891.
[13] E. C. Miller, A. B. Swanson, D. H. Phillips, T. F. Fletcher, J. A. Miller, *Cancer Res.* **1983**, *43*, 1124–1134.
[14] S. Y. Chiang, P. Y. Lee, M. T. Lai, L. C. Shen, W. S. Chung, H. F. Huang, K. Y. Wu, H. C. Wu, *Mutat. Res.* **2011**, *726*, 234–241.
[15] M. K. Qato, T. M. Guenthner, *Toxicol. Lett.* **1995**, *75*, 201–207.
[16] N. Tretyakova, Y. Lin, R. Sangaiah, P. B. Upton, J. A. Swenberg, *Carcinogenesis* **1997**, *18*, 137–147.
[17] T. Munter, L. Cottrell, S. Hill, L. Kronberg, W. P. Watson, B. T. Golding, *Chem. Res. Toxicol.* **2002**, *15*, 1549–1560.
[18] S. Park, J. Hodge, C. Anderson, N. Tretyakova, *Chem. Res. Toxicol.* **2004**, *17*, 1638–1651.
[19] M. Koskinen, P. Vodicka, K. Hemminki, *Chem.-Biol. Interact.* **2000**, *124*, 13–17.
[20] M. Koskinen, K. Plná, *Chem.-Biol. Interact.* **2000**, *129*, 209–229.
[21] D. J. Wood, F. E. Hruska, K. K. Ogilvie, *Can. J. Chem.* **1974**, *52*, 3353–3366.
[22] J. Cadet, R. Ducolomb, F. E. Hruska, *Biochim. Biophys. Acta* **1979**, *563*, 206–215.
[23] R. R. Selzer, A. A. Elfarra, *Chem. Res. Toxicol.* **1996**, *9*, 875–881.
[24] H. Y. H. Kin, J. I. Finneman, C. M. Harris, T. M. Harris, *Chem. Res. Toxicol.* **2000**, *13*, 625–637.
[25] T. Barlow, J. Takeshita, A. Dipple, *Chem. Res. Toxicol.* **1998**, *11*, 838–845.
[26] T. Barlow, J. Ding, P. Vourous, A. Dipple, *Chem. Res. Toxicol.* **1997**, *10*, 1247–1249.
[27] J. Krouželka, I. Linhart, I. Tobrman, *J. Heterocycl. Chem.* **2008**, *45*, 789–795.
[28] R. S. Iyer, M. W. Voehler, T. M. Harries, *J. Am. Chem. Soc.* **1994**, *116*, 8863–8869.
[29] R. M. Silverstein, F. X. Webster, D. J. Kiemle in *Spectrometric Identification of Organic Compounds* (Eds.: D. Brennan, J. Yee, S. Wolfman-Robichaud, S. Rigby), Wiley-VCH, New York, **2005**, pp. 245–285. The interpretation of HMBC spectra requires a degree of flexibility because we do not always find what we expect to find. In particular, depending on the hybridization of carbon and other factors, some of the two-bond ($^2J_{CH}$) or three-bond ($^3J_{CH}$) correlations are occasionally absent. To add to the confusion, we sometimes find four-bond ($^4J_{CH}$) correlations.
[30] S. Balcome, S. Park, D. R. Q. Dorr, L. Hafner, L. Phillips, N. Tretyakova, *Chem. Res. Toxicol.* **2004**, *17*, 950–962.
[31] M. Koskinen, P. Vodicka, K. Hemminki, *Chem.-Biol. Interact.* **2000**, *124*, 13–27.
[32] P. Vodicka, M. Koskinen, M. Arand, F. Oesch, K. Hemminki, *Mutat. Res.* **2002**, *511*, 239–254.
[33] G. J. Latham, L. Zhou, C. M. Harris, T. M. Harris, R. S. Lloyd, *J. Biol. Chem.* **1993**, *268*, 23427–23434.
[34] T. Bastlová, A. Podlutsky, *Mutagenesis* **1996**, *11*, 581–591.
[35] C. R. Noller, P. D. Kneeland, *J. Am. Chem. Soc.* **1946**, *68*, 201–202.
[36] H. R. Mohan, A. S. Rao, *Indian J. Chem. Sect. B* **1998**, *37*, 78–79.
[37] B. Matter, D. Malejka-Giganti, S. Csallany, N. Tretyakova, *Nucleic Acids Res.* **2006**, *34*, 5449–5460.
[38] B. Pang, X. Zhou, H. Yu, M. Dong, K. Taghizadeh, J. S. Wishnok, S. R. Tannenbaum, P. C. Dedon, *Carcinogenesis* **2007**, *28*, 1807–1813.
[39] M. Goggin, C. Anderson, S. Park, J. Swenberg, V. Walker, N. Tretyakova, *Chem. Res. Toxicol.* **2008**, *21*, 1163–1170.

Received: September 22, 2011
Published Online: December 7, 2011

